Vortex Glass and Vortex Liquid in Oscillatory Media

Carolina Brito,[1,2] Igor S. Aranson,[3] and Hugues Chaté[2]

[1]*Instituto de Física, Universidade Federal do Rio Grande do Sul, 91501-970 Porto Alegre, Brazil*
[2]*CEA–Service de Physique de l'Etat Condensé, Centre d'Etudes de Saclay, 91191 Gif-sur-Yvette, France*
[3]*Argonne National Laboratory, 9700 South Cass Avenue, Argonne, Illinois 60439*

(Received 6 August 2002; published 12 February 2003)

We study the disordered, multispiral solutions of two-dimensional oscillatory media for parameter values at which the single-spiral/vortex solution is fully stable. Using the complex Ginzburg-Landau (CGLE) equation, we show that these states, heretofore believed to be static, actually evolve extremely slowly. This is achieved via a reduction of the CGLE to the evolution of the sole vortex coordinates. This true defect-mediated turbulence occurs in two distinct phases, a vortex liquid characterized by normal diffusion of spirals, and a slowly relaxing, intermittent, "vortex glass."

DOI: 10.1103/PhysRevLett.90.068301 PACS numbers: 82.40.Ck, 47.32.Cc, 47.54.+r, 89.75.Kd

Spiral waves are ubiquitous in oscillatory and excitable two-dimensional active media [1]. Their cores are robust wave sources which determine the oscillating frequency of the entire system and may dominate the surrounding dynamics. Spirals (often called vortices) may spontaneously appear and annihilate in a typical manifestation of spatiotemporal chaos. When the single-spiral solution is stable, one easily observes locked, quasifrozen, multispiral disordered structures whose glassy character has been suggested [2–4]. Despite being found in most models of excitable or oscillatory media as well as in experiments (Belousov-Zhabotinskii reaction [5], surface growth [6], and others), surprisingly very little is known about the properties of these disordered states and the transitions leading to their formation.

In this Letter we investigate, in the framework of the complex Ginzburg-Landau equation (CGLE), the general issue of these multispiral solutions and show that they actually evolve on ultraslow time scales. This is achieved thanks both to long numerical simulations of the CGLE and to a quantitatively correct reduction of the dynamics to the evolution of the sole vortex position and phase coordinates. This true defect-mediated turbulence occurs in two distinct phases, a vortex liquid characterized by normal diffusion of individual spirals and a slowly relaxing, intermittent, "vortex glass."

The CGLE describes most properties of generic oscillatory media, at least at a qualitative level, even if one is not in the vicinity of a supercritical long-wavelength Hopf bifurcation, where it can be systematically derived (for reviews, see [7,8]). Under appropriate scaling of the physical variables, it takes the universal form

$$\partial_t A = A - (1 + ic)|A|^2 A + (1 + ib)\Delta A, \qquad (1)$$

where A is a complex amplitude, b and c are real parameters characterizing relative dispersion and nonlinear frequency shift, and Δ is the Laplace operator. Intensive studies revealed a wide variety of striking dynamical phenomena in one, two, and three space dimensions, many of which were also observed in various experimental contexts, sometimes up to a quantitative agreement with CGLE predictions (see, e.g., [9]).

A distinctive feature of the two-dimensional CGLE is the existence of nontrivial sources of spiral waves (vortices) which determine the oscillating frequency of the entire system [10]. The single-spiral solution for a vortex centered at $\mathbf{r}_0$ reads as [11,12]

$$A_s(\mathbf{r}, t) = F(r)\exp\{i[m\theta + \psi(r) + \omega t + \phi]\}, \qquad (2)$$

where $r = |\mathbf{r} - \mathbf{r}_0|$, θ is the polar angle measured from the vortex core, ϕ is an arbitrary phase, and $m = \pm 1$ is the topological charge. Far away from the core, the solution approaches a plane wave with $\psi(r) \simeq kr$, where the asymptotic wave number k is related to the rotation frequency as $\omega = -c - (b - c)k^2$. The dependence of k on b and c is known analytically for $|b - c| \ll 1$ and $|b - c| \gg 1$, e.g., $k \simeq -c^{-1}\exp(-\pi/|2c|)$ for $b = 0$ and $|c| \ll 1$ [11]. In the parameter region where the single-spiral solution is stable and $c \neq b$, the interaction between two well-separated spirals falls off exponentially [12–14]. The screening was attributed to the shock lines where the waves emitted by the cores collide. For relatively small b, c the interaction is monotonic, and the spirals exhibit asymptotic repulsion irrespectively of their charge ("monotonic range") [12,13]. In contrast, for larger b, c satisfying the condition $(c - b)/(1 + bc) > c^* \approx 0.845$ the velocity vs distance dependence is modulated ("oscillatory range"), and the spirals become keen to form a variety of long-living (but unstable) bound states [12,15].

While the above interactions cannot account for the strongly chaotic regimes where many defects are spontaneously generated and undergo violent motion, they are expected to play a leading role in the occurrence of the quasistatic structures of large and small spirals surrounded by a complex network of shocks commonly observed in the large region of the (b, c) parameter space where the single-spiral solution is stable [2–4]. Rather little is known about these cellular structures except that

they seem to be frozen on usual observation time scales. Our results lead to a dramatically different picture.

We conducted detailed numerical studies of the two-dimensional CGLE restricted to the case $b = 0$ and $c > 0$ (for the regimes of interest scaling relations apply in parameter space [8]). The integration domain with periodic boundary conditions was typically of area $S = 512 \times 512$ and the integration time about 10^7. Various integration schemes were used and all results checked against variation of the numerical resolution. We monitored the positions $\mathbf{r}_j(t)$ of all N spirals, the instantaneous "activity" $T = S^{-1} \int_S d\mathbf{r} |\partial_t |A||$, and—when applicable—the spiral diffusion coefficient $D = \frac{1}{Nt} \sum_{j=1}^{N} \langle |\mathbf{r}_j(t) - \mathbf{r}_j(0)|^2 \rangle$. Since, for well-separated spirals, $|A|$ varies only near the cores, T is related to the velocity of spirals.

In the monotonic range $c < c^*$ (Fig. 1), after a short transient during which the initial number of defects may decrease, the number of spirals remains constant and T fluctuates around a well-defined value. In large enough systems, the spiral cores perform normal diffusive motion [Fig. 1(c)]. This *vortex liquid* can be characterized by a viscosity $\nu \sim D^{-1}$. Since all scales, already very large near c^*, diverge exponentially when $c \to 0$, an extensive numerical investigation of the dependence of D on c and on the vortex density $\rho \equiv N/S$ is currently beyond reach.

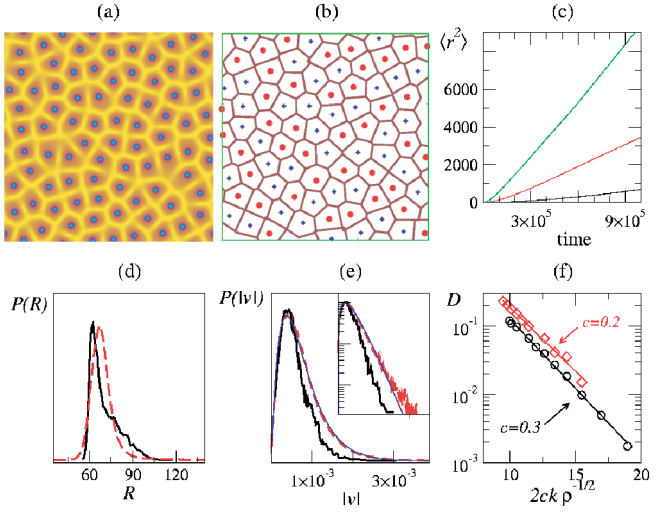

FIG. 1 (color online). (a) Snapshot of $|A|$ for a typical solution of the CGLE at $c = 0.6$ with $N = 82$ spirals ($L = 512$). (b) Core positions and shock lines for a typical solution of Eqs. (6) for the same parameters as in (a). (c) Mean square displacement $\langle r^2 \rangle$ of vortices vs time obtained from CGLE solutions at $c = 0.7$, $L = 256$, and $N = 28, 22, 18$ vortices from top to bottom. (d) Histograms of distance to nearest neighbor $P(R)$ for $c = 0.6$, $N = 82$ ($L = 512$) for the CGLE (solid line) and for solutions of Eqs. (6) (dashed line). (e) Histogram of instantaneous core velocity $P(|v|)$ for $c = 0.7$, $N = 118$ ($L = 512$) for the CGLE (solid line) and for Eqs. (6) (dashed line); the thin line is an exponential fit $P \sim |v| \exp(-\text{const} \times |v|)$. Inset: same data in lin-log scales. (f) D vs $2c|k|/\sqrt{\rho}$ [from solutions of Eqs. (6)], the lines are theoretical fits $D \sim \exp(-c|k|/\sqrt{\rho})$.

Nevertheless, our data indicate that D increases with ρ. The distribution of distances from one spiral core to its nearest-neighbor is peaked at its mean value as expected in a liquid [Fig. 1(d)], but the velocity distribution seems non-Maxwellian [Fig. 1(e) and discussion below].

In contrast, in the oscillatory range $c > c^*$, after a very long transient [Fig. 2(e)], the population of spirals spontaneously segregates into two distinct phases: large and almost immobile spirals and droplets (clusters) of small vortices confined between them [Figs. 2(a) and 2(b); see also [2–4]]. One can thus define a "liquid fraction" of small spirals, whose sizes are typical of the vortex liquid observed in the monotonic range. The first peak in the $P(R)$ histogram corresponds to this liquid fraction [Fig. 2(c)]. In contrast to the vortex liquid, though, $P(R)$ is not well localized and has extra peaks for large R corresponding to the large immobile vortices. When the liquid fraction is small, the resulting state exhibits slow intermittent dynamics (bursts of activity separated by long quiescent intervals reminiscent of glassy dynamics [Fig. 2(d)], whereas for higher fractions the activity T fluctuates around some mean value and the "liquid" vortices can be shown to perform normal diffusion in the space surrounding the big spirals. This picture is typical of phase coexistence in first-order transitions of isolated equilibrium systems [16]. In this respect, our

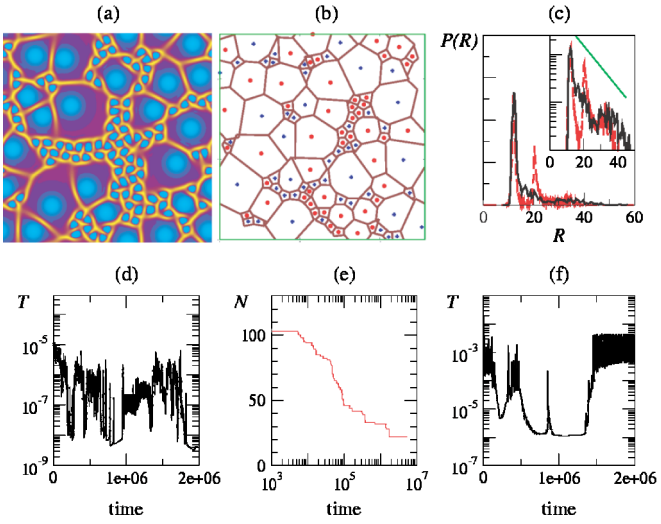

FIG. 2 (color online). Results in the oscillatory range ($c = 1.2$). (a) Snapshot of $|A|$ for a typical solution of the CGLE with $N = 124$ ($L = 256$). (b) Core positions and shock lines for a typical solution of Eqs. (4) [same parameters as in (a)]. (c) Histograms of nearest-neighbor distance $P(R)$ for the CGLE ($L = 512$, $N \simeq 400$, measured around $t = 10^6$ following random initial conditions, solid line) and for solutions of Eqs. (4) ($L = 600$, $N = 700$, dashed line). Inset: same in lin-log scales, with a exponential law (thin line). (d),(e) Time series of the activity T and of the number of vortices N for the evolution of the CGLE in a domain of size $L = 256$ starting from random initial conditions. (f) Same as (d), but from simulations of Eqs. (4) with $N = 100$ vortices (in this case $T \equiv N^{-1} \sum_j |\mathbf{v}_j|$).

results indicate that one can indeed distinguish a "vortex glass" phase. Unfortunately, because of the ever slower time scales over which the system evolves, a precise characterization of this phase using simulations of the CGLE is currently impossible.

To obtain further insight into the problem, we reduced the CGLE to a set of ordinary differential equations describing the motion of the cores $\mathbf{r}_j(t)$ and the phases $\phi_j(t)$ of individual spirals. Only pair interactions are taken into account, making use of the results of [12,15]. The original partial differential equation is thus replaced by a set of $3N$ first-order ordinary differential equations governing the core positions $\mathbf{r}_j(t)$ and the spiral phases $\phi_j(t)$. The phases determine the configuration of the shock lines, which, in turn, yield the velocity of the cores. One clear advantage of this approach, in addition to virtually suppressing physical space, is that it allows one to bypass the ultraslow time scale related to the vanishing value of the wave number k as $c \to 0$.

The problem of the interaction between two oppositely charged spirals is equivalent to that of one spiral and a straight shock line, i.e., a half-plane with the no-flux boundary condition $\partial A/\partial n = 0$. For $c \ll 1$, the equations governing the position and phase of the spiral are

$$\begin{aligned} \frac{dz}{dt} &= 2c^2\pi k(im - cB')\frac{\exp(-2|ck|X)}{\sqrt{\pi|ck|X}}, \\ \dot{\phi} &= 2ck^2\pi\frac{\exp(-2|ck|X)}{\sqrt{\pi|ck|X}}, \end{aligned} \tag{3}$$

where $z = x + iy$ is the (complex) spiral position, $dz/dt = v_x + iv_y$, ϕ is the relative phase, m is the topological charge, $B' \simeq 0.48$, and X is the distance from the core [located at $(-X, 0)$] to the boundary (the y axis is chosen to be on the shock line) [13]. Equations (3) imply the asymptotic repulsion of the spiral from the boundary, in agreement with simulations [12]. This prevents spiral annihilation in the vortex liquid.

The equations in the oscillatory range $c > c^*$ read

$$\begin{aligned} C_x v_x + mC_y v_y &= \frac{-k\sqrt{1-k^2}\exp(-pX)}{\delta\sqrt{2\pi pX}}X^{-\mu}, \\ C_x v_x + mC_y v_y &= \frac{-k\sqrt{1-k^2}\exp(-pX)}{\delta\sqrt{2\pi pX}}X^{-\mu}, \end{aligned} \tag{4}$$

where the complex constants $C_{x,y}, C_0, C_{10}$ are obtained numerically and the real parameters p, μ, δ are derived from the linearized CGLE [12,15]. Equations (4) describe stable bound states of spirals moving along the plane boundary. However, the problem is complicated by the fact that the position of the shock line depends on the relative phase of the spirals. From the condition that the total spiral phases $\Phi_j = \psi(r) + \phi_j \approx -|k|r + \phi_j$ are equal, one finds that the distance to the shock is given by

$$X = |\mathbf{r}_l - \mathbf{r}_j|/2 - (\phi_l - \phi_j)/2|k|. \tag{5}$$

Substituting (5) into Eqs. (4) one finds that the symmetric bound states are unstable in the oscillatory range [15]. Similar phenomena occur for like-charged spirals.

Equations (3) and (4) and condition (5) were used to investigate the dynamics of many-spiral states. In this case, one considers each spiral in the local coordinate system associated with every other spiral and sums up their contributions (details will be published elsewhere). Substituting $r \to 2c|k|r$, $t \to 4\sqrt{2\pi}c^3k^2$, one obtains from Eqs. (3)

$$\begin{aligned} \frac{dz_j}{dt} &= \sum_l (-cB' + im_l)\frac{z_l - z_j}{|z_l - z_j|}\frac{\exp(-X_l)}{\sqrt{X_l}}, \\ \dot{\phi}_j &= \sum_l \frac{\exp(-X_l)}{2c^2\sqrt{X_l}}, \end{aligned} \tag{6}$$

where $X_l = |z_l - z_j|/2 + c(\phi_j - \phi_l)$. A similar rescaling was performed in the oscillatory case.

We investigated numerically and analytically the reduced equations which, in fact, are rather different in the oscillatory range [12,15] and in the monotonic range [13]. Overall quantitative agreement with the full CGLE dynamics has been found.

In the monotonic range in the large enough domain we found liquid behavior accompanied by normal diffusion for all c values. Each spiral core moves chaotically. The nearest-neighbor distance and velocity distributions are in quantitative agreement with those obtained from the full CGLE [Figs. 1(d) and 1(e)], although some deviation is recorded in the tails due to insufficient statistics. The velocity distribution is now clearly exponential [$P \sim |v|\exp(-\text{const} \times |v|)$]: we interpret this strong deviation from the Maxwellian law as a manifestation of the nonequilibrium nature of the vortex liquid. The reason underlying the chaotic behavior is that Eqs. (6) do not obey a variational principle for any c value, due to the nontrivial form of the pairwise interaction. However, an ensemble of like-charged spirals tend to form a stable hexagonal "Wigner" crystal due to mutual repulsion. With periodic boundary conditions (used here), one has an equal mixture of positive and negative spirals, and it can be proved that a square lattice of spirals with alternating charges is unstable in a large system with respect to long-wavelength perturbations. This explains the short-range crystalline order observed [Fig. 1(a)]. The faithfulness of the reduced equations to the CGLE is also testified by the agreement found for the value of the diffusion constant D. For $c = 0.6$, domain size $L = 512$, and $N = 46$ spirals D obtained from CGLE is $D_{\mathrm{CGL}} \approx 0.0033$. For $N = 52$, $D_{\mathrm{CGL}} \approx 0.004\,89$ (error bars are about 10%–15%). Equations (6) yields $D_{\mathrm{ODE}} \approx 0.0036 \pm 0.0002$ for $N = 46$ and $D_{\mathrm{ODE}} \approx 0.0053 \pm 0.0005$ for $N = 52$ [17]. The reduced equations do allow for an extensive study of the asymptotic properties of the vortex liquid. Taking into account that the typical interspiral distance varies like $R \approx 1/\sqrt{\rho}$, one can derive from Eq. (3) that $D \propto \exp(-\chi c|k|/\sqrt{\rho})$ with χ between 1 and 2 ($\chi \to 2$ for

δ-correlated velocities and $\chi \to 1$ in the opposite case). Fits to numerical results yield $\chi \approx 1$ [Fig. 1(f)].

In the oscillatory range also, the reduced equations faithfully reproduce the phenomenology of symmetry breaking, intermittent activity at low vortex densities, and vortex glass formation observed in the CGLE [Figs. 2(d) and 2(f)]. The distance distribution function obtained from Eqs. (4) also is in qualitative agreement with the full CGLE results, Fig. 2(c) (discrepancy is likely due to insufficient statistics for the full CGLE data). Moreover, the peak population seems to be exponentially distributed, indicating the nonzero probability of the existence of a large spiral which will determine the ultraslow time scale of the system. The reduced equations provide an interesting framework to discuss the mechanisms leading to intermittent dynamics in the vortex glass containing liquid droplets. For a spiral embedded in a large domain of arbitrary shape, Eqs. (4) generally do not have a stationary solution $\mathbf{v}_j = \dot{\boldsymbol{\phi}}_j = 0$ for all j (because the complex constants $C_{x,y}$ and $C_{10,0}$ are typically not proportional). As a result, it is impossible to satisfy the conditions $\mathbf{v}_j = 0$ and $\dot{\boldsymbol{\phi}}_j = 0$ simultaneously. The drift of the spirals changes the phases and, therefore, the shape of their domains. When the phase difference becomes large enough, the shock lines rearrange and trigger rapid dynamics within the liquid droplets. Since the velocity of the cores is an exponential function of interspiral separation, the typical time scale between such rapid rearrangements is exponentially large in the spiral size.

We have found that the transition from vortex liquid to vortex glass possesses some features of a first-order phase transition. More work is needed to elucidate the corresponding phase diagram. Returning to the question of the possibility of "true" glassy dynamics [18] (as testified, e.g., by some aging phenomena), several comments are now in order. Preliminary numerical results of the reduced equations in very large systems at low vortex density indicate that the intermittent space-time activity usually reaches a self-averaging asymptotic regime, in contrast with spin-glass–type behavior [19] and in closer agreement with a structural glass, which can be viewed sometimes as a very viscous fluid. On the other hand, these regimes, as far as they can be studied for the full CGLE, do exhibit a slow, possibly aginglike, decay of the number of vortices in the system [Fig. 2(e)]. This leaves the door open for an actual vortex glass in this fully deterministic, noiseless, disorder-free context — a challenge to models of glassy behavior in statistical physics.

Our work has shown that the multispiral "frozen" states of the CGLE actually evolve on very long time scales. These ultraslow regimes are relevant, we believe, to the many related models and experimental situations. A vortex liquid and a vortex glass can be distinguished depending on the effective interaction law between spirals. These "phases" are dynamical, and are remarkably well accounted for, in the case of the CGLE, by a reduction of the full problem to a finite set of ordinary differential equations governing the vortex cores. This constitutes maybe the first success for the ideas underlying the concept of "defect-mediated turbulence" put forward in the 1980s [8,20,21].

This work was supported by the U.S. Department of Energy under Contract No. W-31-109-ENG-38.

[1] A. T. Winfree, *When Time Breaks Down* (Princeton University Press, Princeton, NJ, 1987); A. Goldbeter, *Biochemical Oscillations and Cellular Rhythms* (Cambridge University Press, Cambridge, 1996).
[2] G. Huber, P. Alstrøm, and T. Bohr, Phys. Rev. Lett. **69**, 2380 (1992).
[3] T. Bohr, G. Huber, and E. Ott, Europhys. Lett. **33**, 589 (1996).
[4] H. Chaté and P. Manneville, Physica (Amsterdam) **224A**, 348 (1996).
[5] Q. Ouyang and J.-M. Flesselles, Nature (London) **379**, 143 (1996).
[6] M. Hawley, I. D. Raistrick, J. G. Beery, and R. J. Houlton, Science **251**, 1587 (1991); I. S. Aranson, A. R. Bishop, I. Daruka, and V. M. Vinokur, Phys. Rev. Lett. **80**, 1770 (1998).
[7] M. Cross and P. C. Hohenberg, Rev. Mod. Phys. **65**, 851 (1993).
[8] I. S. Aranson and L. Kramer, Rev. Mod. Phys. **74**, 99 (2002).
[9] J. Burguete, H. Chaté, F. Daviaud, and N. Mukolobwiez, Phys. Rev. Lett. **82**, 3252 (1999).
[10] Y. Kuramoto, *Chemical Oscillations, Waves and Turbulence* (Springer, Berlin, 1984).
[11] P. S. Hagan, SIAM J. Appl. Math. **42**, 762 (1982).
[12] I. S. Aranson, L. Kramer, and A. Weber, Phys. Rev. E **47**, 3231 (1993).
[13] V.N. Biktashev, *Nonlinear Waves II*, edited by A.V. Gaponov-Grekhov and M. I. Rabinovich, Research Reports in Physics (Springer, Heidelberg, 1989).
[14] L. M. Pismen and A. A. Nepomnyashchy, Phys. Rev. A **44**, R2243 (1991).
[15] I. S. Aranson, L. Kramer, and A. Weber, Phys. Rev. E **48**, R9 (1993).
[16] A. J. Bray, Adv. Phys. **43**, 357 (1994).
[17] Extensive comparison with the CGLE is hampered by the fact that a long-enough run with reliable resolution takes about 1 month of CPU time on a fast workstation, even for $c = 0.6$–0.7. For smaller c, such simulations are practically impossible.
[18] See, e.g., C. A. Angell, Science **267**, 1924 (1995).
[19] K. H. Fischer and J. A. Hertz, *Spin Glasses* (Cambridge University Press, London, 1991).
[20] P. Coullet, L. Gil, and J. Lega, Phys. Rev. Lett. **62**, 1619 (1989).
[21] Kosterlitz-Thouless-like transition in the noisy CGLE is discussed in I. S. Aranson, H. Chaté, and L.-H. Tang, Phys. Rev. Lett. **80**, 2646 (1998).